PHYSICAL REVIEW B VOLUME 38, NUMBER 14 15 NOVEMBER 1988-I

Influence of electron-hole scattering on subpicosecond carrier relaxation in $Al_xGa_{1-x}As/GaAs$ quantum wells

Stephen M. Goodnick
Center for Advanced Materials Research, Oregon State University, Corvallis, Oregon 97331

Paolo Lugli
Dipartimento di Ingegneria Meccanica, II Università di Roma, Via Orazio Raimondo, 00173 Roma, Italy

(Received 20 June 1988)

We have simulated subpicosecond-time-scale pump-and-probe absorption experiments in $Al_xGa_{1-x}As/GaAs$ quantum wells using an ensemble Monte Carlo calculation of the photoexcited electron-hole system. For excess carrier energies less than the optical-phonon energy, our results show that the apparent 200-fs relaxation observed in differential transmission experiments is directly attributable to relaxation of electrons through electron-electron scattering with inelastic electron-hole scattering playing a smaller role. Photoexcited holes are found to thermalize on a 50-fs time scale which is much shorter than the relaxation time of the electrons. However, a nonthermal hole distribution develops *after* the pulse due to optical-phonon absorption at 300 K which should give rise to absorption features at higher photon energies.

Time-resolved optical studies of photoexcitation in semiconductors have provided a unique probe of nonequilibrium carrier relaxation processes in semiconductors on a picosecond and subpicosecond time scale.[1-5] In the experiments of Knox and co-workers[4,5] pump-and-probe absorption spectroscopy was used to study the relaxation kinetics of optically excited carriers in undoped[4] and modulation-doped[5] quantum wells. For nonexcitonic band-to-band absorption, the absorption coefficient depends on the number of occupied initial states and the number of unoccupied final states. For low-level excitation, the differential transmission, $\Delta T/T_0$, is equal to the sum of electron and hole distributions

$$\Delta T(h\nu,t)/T_0 = f_e(\mathbf{k},t)+f_h(\mathbf{k},t)\,, \tag{1}$$

where $f_e(\mathbf{k},t)$ and $f_h(\mathbf{k},t)$ are the time-dependent electron and hole distribution functions for a wave vector $\mathbf{k}$ corresponding to a photon energy of $h\nu$. In the experiments of Knox and co-workers, the pump energy was chosen such that the electron excess energy, $\Delta E_c = h^2k^2/2m_e$, was less than the optical-phonon energy. A peak in the differential transmission was observed centered at the pump-probe energy which was attributed to absorption saturation due to a nonequilibrium distribution of photogenerated electrons and holes. Two hundred femtoseconds after the peak of the pump pulse, the differential transmission spectrum was observed to relax to a Maxwellian line shape. The observed relaxation in the differential transmission spectra was therefore argued to result from electron-electron scattering as optical-phonon emission was prohibited. To the extent in which this experiment simulates the time evolution of an isolated system (i.e., no energy transfer to the lattice and constant particle number after the pulse), the observed relaxation after the pulse is a direct consequence of Boltzmann's H theorem[6] which predicts that an interacting system of particles in an arbitrary initial distribution will evolve along a path of increasing entropy in phase space toward the equilibrium state characterized by a Maxwell-Boltzmann distribution (or Fermi-Dirac at high density).

Monte Carlo simulations of the results of Knox and co-workers[4,5] have been performed for the electron system alone which showed that this relaxation could be explained by electron-electron scattering.[7-9] However, in all such optical experiments, comparable numbers of electrons and holes are present which complicates the analysis since relaxation of the hole distribution contributes to the differential transmission in (1), and inelastic electron-hole scattering is present which may dominate the carrier-carrier scattering.

In order to understand the role that holes play in the apparent carrier relaxation in ultrafast laser experiments, we have included the dynamics of holes into a Monte Carlo simulation of quantum-well systems described in detail elsewhere.[10] We have neglected the complications of band mixing in the hole states[11] and simply considered a square-well potential for heavy-hole states within the effective-mass approximation. Hole generation within the light-hole subbands is neglected due to the lower density of states, and the heavy-hole-to-light-hole transitions are assumed negligible on the time scale of these experiments. Unscreened polar-optical-phonon (POP) scattering and transverse-optical (TO) scattering are included for the holes along with impurity and carrier-carrier scattering (CCS). For TO phonon scattering within the quantized hole system, we use the optical deformation potential scattering rate as calculated by Ridley[12] for quasi-two-dimensional systems. We treat intercarrier scattering through a screened Coulomb interaction as before[8-10] with the effective mass replaced with a reduced mass

$$m_r = 2m_im_j/(m_i+m_j)\,, \tag{2}$$

where m_i and m_j are the effective masses of band i and band j which reduces to the intraband mass for $i=j$. We

consider only long-wavelength diagonal screening derived from the matrix random-phase approximation (RPA) as before:[8]

$$\epsilon_D(q) = 1 + \sum_{i,n} q_{in} \frac{f_{in}(0)}{q} , \tag{3}$$

where n is the band index (electrons, heavy holes, etc.) and i is the subband index within each band. The constant q_{in} is given by

$$q_{in} = m_{in}^*/\pi\hbar^2(2\pi e^2/\epsilon_{sc}) , \tag{4}$$

with ϵ_{sc} the semiconductor dielectric constant. The occupancy, $f_{in}(0)$, of the bottom of the band is calculated at every time step (5 fs) during the simulation and used to update the CCS rate which changes dynamically during photoexcitation.

In the present communication, we simulate the earlier experiments of Knox *et al.*[4] corresponding to an undoped, 95-Å-wide quantum well with an injected carrier density of 2×10^{10} cm^{-2}. A background density of 2×10^9/cm^2 is assumed for the unintentional doping in the molecular-beam-epitaxial (MBE) layer which is also taken as the ionized-impurity-scattering density. At these low values of the free-carrier and ionized-impurity concentrations, square-well solutions to the Schrödinger equation are virtually identical to those calculated using self-consistent wave functions. We assume a 100-fs laser-pulse duration with a spectral width of 20 meV. As described elsewhere,[10] particles are added to the Monte Carlo simulation in accordance to the temporal and energy dependencies of the pump probe in order to simulate laser excitation. Typically, we use 20000–40000 particles and a 5-fs time step in order to assure the statistical accuracy of the results. We neglect the photon momentum in the optical transition so that electrons and holes are added simultaneously with the same wave vector. Therefore, a certain correlation exists in the initial distribution between electrons and holes which rapidly decays through elastic and inelastic collisions.

Figure 1 shows the simulated results at 300 K for electrons and holes in which the excess energy of the electrons above the conduction band edge is 20 meV corresponding to the experimental conditions of Ref. 4. We plot the average energy of electrons and holes as a function of time during and after the pulse where the peak of the pulse occurs at $t = 200$ ps. Both electrons and holes are injected with excess energies below the lattice temperature, with the heavy holes injected at a much lower temperature than electrons due to the large difference in the density of states. A substantial heating of the hole distribution occurs during the first 200 fs after the pulse peak due to TO and POP phonon absorption. A weaker heating of the holes due to inelastic electron-hole scattering is also present. Simulated results with the same model at low temperature show that at least 1 ps is required for the electrons and holes to equilibrate with one another through CCS, which is much longer than the 200-fs heating shown in Fig. 1. Experimentally, lower temperatures are required to completely isolate the effects of intercarrier scattering from that of lattice vibrations.

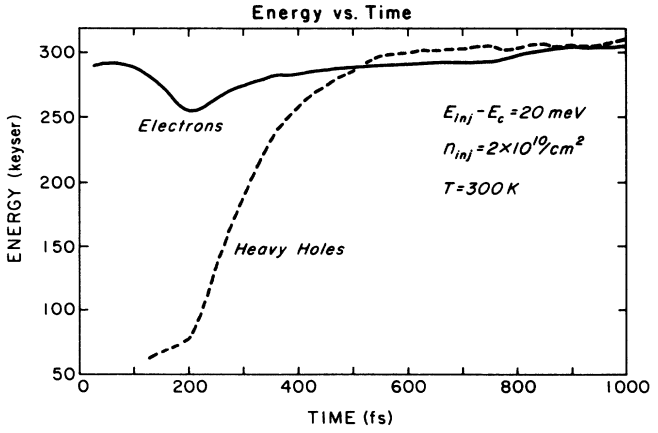

FIG. 1. Energy vs time for electrons and holes at 300 K. The pulse duration is 100 fs and peaks at $t = 200$ fs.

In Fig. 2 we plot the instantaneous electron-energy distribution at various times before and after the pulse. An athermal, Gaussian-shaped pulse is observed at time zero which subsequently evolves to a Maxwellian-shaped pulse after 200 fs. The evolution of the electron distribution in Fig. 2 is qualitatively similar to that observed experimentally over the same time scale in the differential transmission spectra. As suggested by Fig. 1, considerable phonon emission and absorption occur at 300 K which complicates the interpretation of the relaxation. Carrier relaxation is driven by inelastic scattering which allows the system to "sample" various regions of phase space. Optical-phonon scattering alone cannot account for the observed relaxation to an equilibrium distribution as the carriers would then simply scatter back and forth between the same constant energy shells separated by $\hbar\omega_0$. By tabulating the energy exchanged per scattering event as a function of time, we are able to determine which scattering mechanism is responsible for relaxation. Energy exchange due to electron-electron scattering was found to be two to three times that of electron-hole and POP phonon scattering on the time scale of Fig. 2 which suggests the former mechanism as the primary driving force for relaxation. Our previous results for electrons alone at low temperature show the same qualitative relaxation over the same time scale which further supports this conclusion.[8,9]

In Fig. 3 we show a similar plot to Fig. 2 for the heavy-hole energy distribution function. The relaxation of the hole distribution occurs within 50 fs which is much sooner than that of the electrons. This difference is due to the larger intercarrier scattering rate corresponding to the larger effective hole mass and due to the fact that holes are injected much closer to the band edge. Perhaps more interesting in Fig. 3 is the appearance of an athermal phonon replica (at 40 meV) in the hole distribution due to TO and POP absorption which peaks after the maximum of the laser pulse. Such a feature has not been observed in previous experimental studies. However, the photon energy which couples this excess hole energy to the conduction band is in excess of 1.7 eV (based on a parabolic band model) which is outside the optically coupled region of

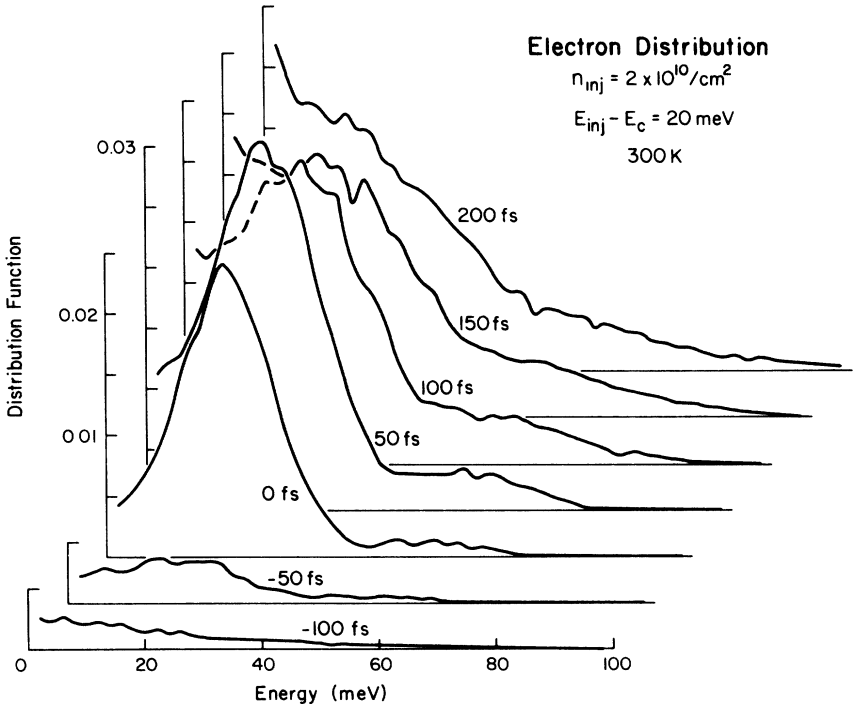

FIG. 2. Electron distribution function as a function of energy at various times before and after a pump pulse at time $t = 0$.

those experiments. Time-resolved observation of this feature in absorption experiments could provide a direct measure of the hole-optical-phonon coupling and possible nonequilibrium phonon effects at lower temperatures. As shown in Fig. 3, the athermal phonon replica is observed to smear out with time due to hole-hole scattering and eventually form a Maxwellian tail after 200 fs.

Finally, in Fig. 4 we plot the differential transmission spectra as a function of photon energy at various times using Eq. (2) and the results of Figs. 2 and 3. The excess energies of f_e and f_h coupled by a photon of energy $h\nu$ are chosen to satisfy the momentum conservation rules for band-to-band optical transitions. A quantitative comparison between Fig. 4 and experimental spectra[4,5] is difficult at this time due to the overlap of the excitonic absorption spectrum at low energies which changes dynamically dur-

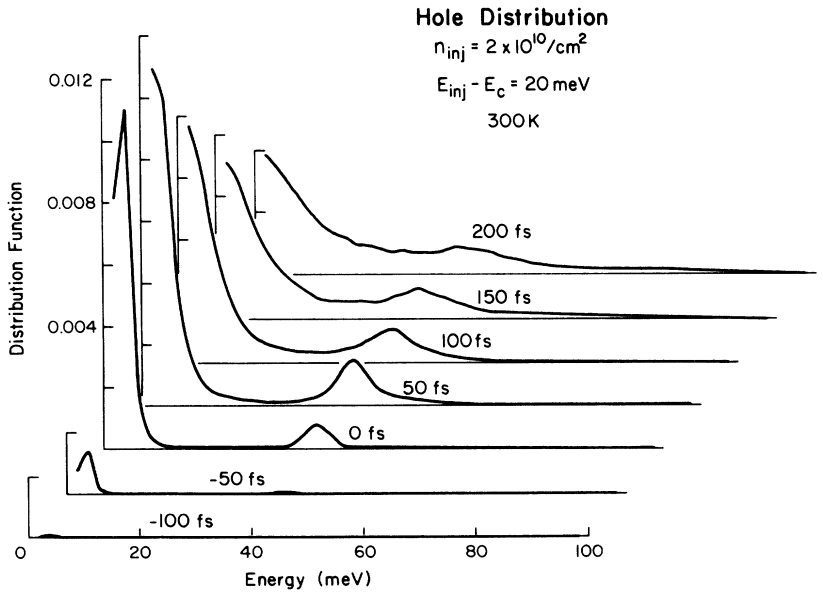

FIG. 3. Hole distribution function as a function of energy at various times during a pump pulse at $t = 0$.

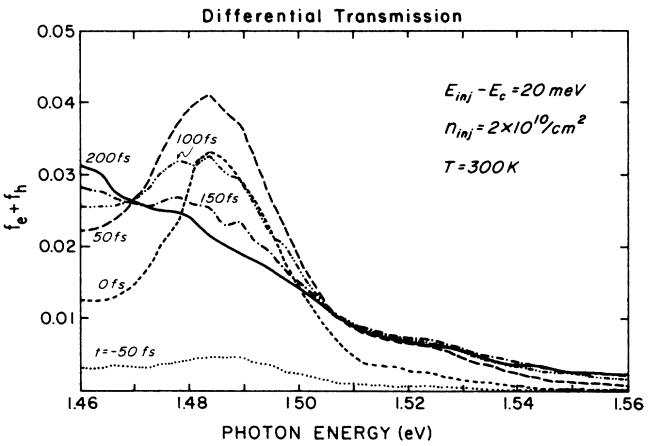

FIG. 4. Differential transmission based on the distribution functions of Figs. 2 and 3 at the same times.

ing photoexcitation.[13] The evolution of the calculated differential transmission spectrum in Fig. 4 is seen to follow that of the electron distribution of Fig. 2 and not that of the holes in Fig. 3 which relaxes much faster. This result supports the original conjecture of Knox *et al.*[4] that their results measured the relaxation of the electron distribution function, at least for the present set of experimental conditions.

In conclusion, our Monte Carlo results for a photoexcited electron-hole plasma in semiconductor quantum wells show that the time-dependent relaxation observed in experimental differential transmission spectra is primarily due to relaxation of the electron distribution. The mechanism for this relaxation is principally through inelastic electron-electron scattering with a lesser contribution due to electron-hole scattering. At 300 K an athermal phonon replica in the hole distribution appears due to POP and TO phonon absorption which should result in absorption spectrum features at large phonon energies. The time evolution of this feature depends strongly on the hole-phonon absorption time as well as hole-hole scattering which broadens this short-time distribution into a thermal tail after several hundred femtoseconds.

The authors would like to thank D. S. Chemla and W. H. Knox for helpful discussions related to this work. The research was supported under the U.S. Office of Naval Research Contract No. N00014-87-K-0686.

[1]J. F. Ryan, R. A. Taylor, A. J. Turberfield, and J. M. Worlock, Surf. Sci. **170**, 511 (1986).

[2]D. Y. Oberli, D. R. Wake, M. V. Klein, J. Klem, T. Henderson, and H. Morkoc, Phys. Rev. Lett. **59**, 696 (1987).

[3]M. Rosker, F. Wise, and C. L. Tang, Appl. Phys. Lett. **49**, 1714 (1986).

[4]W. H. Knox, C. Hirlimann, D. A. B. Miller, J. Shah, D. S. Chemla, and C. V. Shank, Phys. Rev. Lett. **56**, 1191 (1986).

[5]W. H. Knox, D. S. Chemla, and G. Livescu, Solid State Electron. **31**, 425 (1988).

[6]See, for example, R. C. Tolman, *The Principles of Statistical Mechanics* (Oxford Univ. Press, London, 1938), pp. 134–177.

[7]D. W. Bailey, M. Artaki, C. Stanton, and K. Hess, J. Appl. Phys. **62**, 4639 (1987).

[8]S. M. Goodnick and P. Lugli, Appl. Phys. Lett. **51**, 585 (1987).

[9]S. M. Goodnick and P. Lugli, Solid State Electron. **31**, 463 (1988).

[10]S. M. Goodnick and P. Lugli, Phys. Rev. B **37**, 2578 (1988).

[11]M. Altarelli, in *Heterojunctions and Semiconductor Superlattices,* edited by G. Allan, G. Bastard, N. Boccara, M. Lannoo, and M. Voos (Springer-Verlag, Berlin, 1986), pp. 12–37.

[12]B. K. Ridley, J. Phys. C **15**, 5899 (1982).

[13]S. Schmitt-Rink, D. S. Chemla, and D. A. B. Miller, Phys. Rev. B **32**, 6601 (1985).